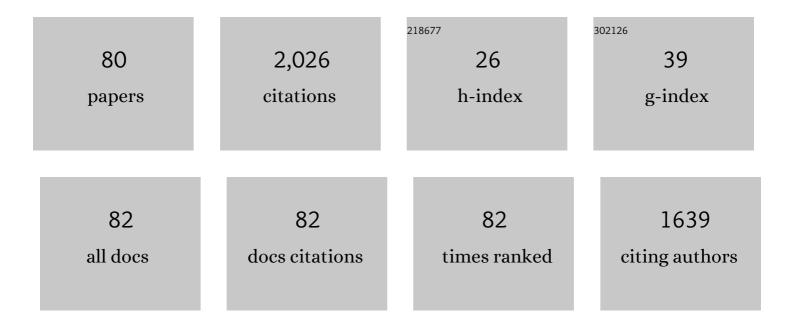
Sarah A Gleeson

List of Publications by Year in descending order

Source: https://exaly.com/author-pdf/4940028/publications.pdf Version: 2024-02-01



#	Article	IF	CITATIONS
1	Biogenic and abiogenic low-Mg calcite (bLMC and aLMC): Evaluation of seawater-REE composition, water masses and carbonate diagenesis. Chemical Geology, 2011, 280, 180-190.	3.3	129
2	The Mineralogy and Geochemistry of the Cerro Matoso S.A. Ni Laterite Deposit, Montelibano, Colombia. Economic Geology, 2004, 99, 1197-1213.	3.8	84
3	Open system sulphate reduction in a diagenetic environment – Isotopic analysis of barite (δ34S and δ18O) and pyrite (δ34S) from the Tom and Jason Late Devonian Zn–Pb–Ba deposits, Selwyn Basin, Canada. Geochimica Et Cosmochimica Acta, 2016, 180, 146-163.	3.9	77
4	Zebra dolomitization as a result of focused fluid flow in the Rocky Mountains Fold and Thrust Belt, Canada. Sedimentology, 2005, 52, 1067-1095.	3.1	70
5	Coupled partitioning of Au and As into pyrite controls formation of giant Au deposits. Science Advances, 2019, 5, eaav5891.	10.3	64
6	The origin and evolution of base metal mineralising brines and hydrothermal fluids, South Cornwall, UK. Geochimica Et Cosmochimica Acta, 2001, 65, 2067-2079.	3.9	55
7	Trace Element Geochemistry of Magnetite and Its Relationship to Cu-Bi-Co-Au-Ag-U-W Mineralization in the Great Bear Magmatic Zone, NWT, Canada. Economic Geology, 2014, 109, 1901-1928.	3.8	54
8	Infiltration of basinal fluids into high-grade basement, South Norway: sources and behaviour of waters and brines. Geofluids, 2003, 3, 33-48.	0.7	53
9	Intracratonic crustal seawater circulation and the genesis of subseafloor zinc-lead mineralization in the Irish orefield. Geology, 2005, 33, 805.	4.4	50
10	The source of halogens in geothermal fluids from the Taupo Volcanic Zone, North Island, New Zealand. Geochimica Et Cosmochimica Acta, 2014, 126, 265-283.	3.9	49
11	The sources and evolution of mineralising fluids in iron oxide–copper–gold systems, Norrbotten, Sweden: Constraints from Br/Cl ratios and stable Cl isotopes of fluid inclusion leachates. Geochimica Et Cosmochimica Acta, 2009, 73, 5658-5672.	3.9	48
12	Hydrothermal fluid evolution and metal transport in the Kiruna District, Sweden: Contrasting metal behaviour in aqueous and aqueous–carbonic brines. Geochimica Et Cosmochimica Acta, 2013, 102, 89-112.	3.9	48
13	Origin of retrograde fluids in metamorphic rocks. Journal of Geochemical Exploration, 2000, 69-70, 281-285.	3.2	45
14	Re-Os dating of pyrite confirms an early diagenetic onset and extended duration of mineralization in the Irish Zn-Pb ore field. Geology, 2015, 43, 143-146.	4.4	44
15	Cl/Br ratios and stable chlorine isotope analysis of magmatic–hydrothermal fluid inclusions from Butte, Montana and Bingham Canyon, Utah. Mineralium Deposita, 2009, 44, 837-848.	4.1	39
16	Mineralogical characterization of the Nkamouna Co–Mn laterite ore, southeast Cameroon. Mineralium Deposita, 2013, 48, 155-171.	4.1	39
17	Partitioning of arsenic between hydrothermal fluid and pyrite during experimental siderite replacement. Chemical Geology, 2018, 500, 136-147.	3.3	39
18	Using zircon trace element composition to assess porphyry copper potential of the Guichon Creek batholith and Highland Valley Copper deposit, south-central British Columbia. Mineralium Deposita, 2021, 56, 215-238.	4.1	38

#	Article	IF	CITATIONS
19	Gold Refining by Bismuth Melts in the Iron Oxide-Dominated NICO Au-Co-Bi (ÂCuÂW) Deposit, NWT, Canada. Economic Geology, 2015, 110, 291-314.	3.8	36
20	The thermal and chemical evolution of hydrothermal vent fluids in shale hosted massive sulphide (SHMS) systems from the MacMillan Pass district (Yukon, Canada). Geochimica Et Cosmochimica Acta, 2016, 193, 251-273.	3.9	32
21	New U-Pb constraints on the age of the Little Dal Basalts and Gunbarrel-related volcanism in Rodinia. Precambrian Research, 2017, 296, 168-180.	2.7	31
22	Postâ€magmatic hydrothermal circulation and the origin of base metal mineralization, Cornwall, UK. Journal of the Geological Society, 2000, 157, 589-600.	2.1	30
23	A Paleoproterozoic Andean-type iron oxide copper-gold environment, the Great Bear magmatic zone, Northwest Canada. Ore Geology Reviews, 2017, 81, 123-139.	2.7	29
24	On the occurrence and wider implications of anomalously low ÎD fluids in quartz veins, South Cornwall, England. Chemical Geology, 1999, 160, 161-173.	3.3	28
25	Fluids associated with hydrothermal dolomitization in St. George Group, western Newfoundland, Canada. Geofluids, 2010, 10, 422-437.	0.7	28
26	Fluid inclusion constraints on the origin of the brines responsible for Pb?Zn mineralization at Pine Point and coarse non-saddle and saddle dolomite formation in southern Northwest Territories. Geofluids, 2007, 7, 51-68.	0.7	27
27	Origin of the Breno and Esino dolomites in the western Southern Alps (Italy): Implications for a volcanic influence. Marine and Petroleum Geology, 2016, 69, 38-52.	3.3	27
28	Petroleum infiltration of high-grade basement, South Norway: Pressure-Temperature-time-composition (P-T-t-X) constraints. Geofluids, 2002, 2, 41-53.	0.7	26
29	Garnet U-Pb dating of the Yinan Au-Cu skarn deposit, Luxi District, North China Craton: Implications for district-wide coeval Au-Cu and Fe skarn mineralization. Ore Geology Reviews, 2020, 118, 103310.	2.7	26
30	A basement-interacted fluid in the N81 deposit, Pine Point Pb-Zn District, Canada: Sr isotopic analyses of single dolomite crystals. Mineralium Deposita, 2012, 47, 749-754.	4.1	25
31	The origin of Late Devonian (Frasnian) stratiform and stratabound mudstone-hosted barite in the Selwyn Basin, Northwest Territories, Canada. Marine and Petroleum Geology, 2017, 85, 1-15.	3.3	24
32	A NEW SUBSEAFLOOR REPLACEMENT MODEL FOR THE MACMILLAN PASS CLASTIC-DOMINANT Zn-Pb $\hat{A}\pm$ Ba DEPOSITS (YUKON, CANADA). Economic Geology, 2020, 115, 953-959.	3.8	24
33	Thermochemical sulphate reduction in the Upper Devonian Cairn Formation of the Fairholme carbonate complex (Southâ€West Alberta, Canadian Rockies): evidence from fluid inclusions and isotopic data. Sedimentology, 2009, 56, 439-460.	3.1	23
34	Timing and thermochemical constraints on multi-element mineralisation at the Nori/RA Cu–Mo–U prospect, Great Bear magmatic zone, Northwest Territories, Canada. Mineralium Deposita, 2010, 45, 549-566.	4.1	23
35	The origin of sulfate mineralization and the nature of the BaSO4–SrSO4 solid-solution series in the Ain Allega and El Aguiba ore deposits, Northern Tunisia. Ore Geology Reviews, 2012, 48, 165-179.	2.7	23
36	Determination of the origin of salinity in granite-related fluids: evidence from chlorine isotopes in fluid inclusions. Journal of Geochemical Exploration, 2000, 69-70, 309-312.	3.2	22

#	Article	IF	CITATIONS
37	Evidence of multiple halogen sources in scapolites from iron oxide-copper-gold (IOCC) deposits and regional Na Cl metasomatic alteration, Norrbotten County, Sweden. Chemical Geology, 2017, 451, 90-103.	3.3	22
38	From exploration to remediation: A microbial perspective for innovation in mining. Earth-Science Reviews, 2021, 216, 103563.	9.1	22
39	Regional Fluid Flow and Gold Mineralization in the Dalradian of the Sperrin Mountains, Northern Ireland. Economic Geology, 2000, 95, 1389-1416.	3.8	22
40	The high-temperature behavior of defect hydrogen species in quartz: Implications for hydrogen isotope studies. American Mineralogist, 2003, 88, 262-270.	1.9	21
41	Massive sulfide Zn deposits in the Proterozoic did not require euxinia. Geochemical Perspectives Letters, 0, , 19-24.	5.0	20
42	Links between seawater paleoredox and the formation of sediment-hosted massive sulphide (SHMS) deposits — Fe speciation and Mo isotope constraints from Late Devonian mudstones. Chemical Geology, 2018, 490, 45-60.	3.3	19
43	Genesis of the Paleoproterozoic NICO iron oxide–cobalt–gold–bismuth deposit, Northwest Territories, Canada: Evidence from isotope geochemistry and fluid inclusions. Precambrian Research, 2015, 268, 168-193.	2.7	18
44	Spatio-temporal evolution of ocean redox and nitrogen cycling in the early Cambrian Yangtze ocean. Chemical Geology, 2020, 554, 119803.	3.3	18
45	Geochemical constraints on the origin of the Kicking Horse and Monarch Mississippi Valley-type lead-zinc ore deposits, southeast British Columbia, Canada. Mineralium Deposita, 2007, 42, 913-935.	4.1	17
46	Petrography, Mineralogy, and Geochemistry of the Nkamouna Serpentinite: Implications for the Formation of the Cobalt-Manganese Laterite Deposit, Southeast Cameroon. Economic Geology, 2012, 107, 25-41.	3.8	17
47	The Importance of Siliceous Radiolarian-Bearing Mudstones in the Formation of Sediment-Hosted Zn-Pb ű Ba Mineralization in the Selwyn Basin, Yukon, Canada. Economic Geology, 2015, 110, 2139-2146.	3.8	16
48	From basin to basement: the movement of surface fluids into the crust. Journal of Geochemical Exploration, 2000, 69-70, 527-531.	3.2	15
49	Sulfur Isotope Constraints on the Conditions of Pyrite Formation in the Paleoproterozoic Urquhart Shale Formation and George Fisher Zn-Pb-Ag Deposit, Northern Australia. Economic Geology, 2020, 115, 1003-1020.	3.8	15
50	Regional Fluid Flow and Gold Mineralization in the Dalradianof the Sperrin Mountains, Northern Ireland. Economic Geology, 2000, 95, 1389-1416.	3.8	14
51	The carbonate-hosted willemite prospects of the Zambezi Metamorphic Belt (Zambia). Mineralium Deposita, 2011, 46, 707-729.	4.1	14
52	Characterization and dispersal of indicator minerals associated with the Pine Point Mississippi Valley-type (MVT) district, Northwest Territories, Canada. Canadian Journal of Earth Sciences, 2015, 52, 776-794.	1.3	14
53	Differentiating between hydrothermal and diagenetic carbonate using rare earth element and yttrium (REE+Y) geochemistry: a case study from the Paleoproterozoic George Fisher massive sulfide Zn deposit, Mount Isa, Australia. Mineralium Deposita, 2022, 57, 187-206.	4.1	14
54	Micro-Fourier Transform Infrared (FT-IR) and ÎƊ value investigation of hydrothermal vein quartz: Interpretation of fluid inclusion ÎƊ values in hydrothermal systems. Geochimica Et Cosmochimica Acta, 2008, 72, 4595-4606.	3.9	13

#	Article	IF	CITATIONS
55	Variability of outcrop magnetic susceptibility and its relationship to the porphyry Cu centers in the Highland Valley Copper district. Ore Geology Reviews, 2019, 107, 201-217.	2.7	13
56	RECOGNIZING PORPHYRY COPPER POTENTIAL FROM TILL ZIRCON COMPOSITION: A CASE STUDY FROM THE HIGHLAND VALLEY PORPHYRY DISTRICT, SOUTH-CENTRAL BRITISH COLUMBIA. Economic Geology, 2021, 116, 1035-1045.	3.8	13
57	Development of secondary porosity in the Fairholme carbonate complex (southwest Alberta, Canada). Journal of Geochemical Exploration, 2006, 89, 394-397.	3.2	12
58	More than a trace of oxygen: Ichnological constraints on the formation of the giant Zn-Pb-Ag ± Ba deposits, Red Dog district, Alaska. Geology, 2015, 43, 867-870.	4.4	12
59	Mineralogical and Isotopic Characteristics of Sodic-Calcic Alteration in the Highland Valley Copper District, British Columbia, Canada: Implications for Fluid Sources in Porphyry Cu Systems. Economic Geology, 2020, 115, 841-870.	3.8	12
60	Three-Dimensional and Microstructural Fingerprinting of Gold Nanoparticles at Fluid-Mineral Interfaces. American Mineralogist, 2021, 106, 97-104.	1.9	12
61	Surface-derived fluids in basement rocks:inferences from palaeo-hydrothermal systems. Journal of Geochemical Exploration, 2003, 78-79, 61-65.	3.2	11
62	The Mineralogical Evolution of the Clastic Dominant-Type Zn-Pb ± Ba Deposits at Macmillan Pass (Yukon, Canada)—Tracing Subseafloor Barite Replacement in the Layered Mineralization. Economic Geology, 2020, 115, 961-979.	3.8	11
63	The Teena Zn-Pb Deposit (McArthur Basin, Australia). Part II: Carbonate Replacement Sulfide Mineralization During Burial Diagenesis—Implications for Mineral Exploration. Economic Geology, 2021, 116, 1769-1801.	3.8	11
64	The Teena Zn-Pb Deposit (McArthur Basin, Australia). Part I: Syndiagenetic Base Metal Sulfide Mineralization Related to Dynamic Subbasin Evolution. Economic Geology, 2021, 116, 1743-1768.	3.8	10
65	Improved detection limits for transient signal analysis of fluid inclusions by inductively coupled plasma atomic emission spectrometry using correlated background correction. Analyst, The, 1995, 120, 1421.	3.5	9
66	Linking Mineralogy to Lithogeochemistry in the Highland Valley Copper District: Implications for Porphyry Copper Footprints. Economic Geology, 2020, 115, 871-901.	3.8	9
67	The Formation of Highly Positive δ34S Values in Late Devonian Mudstones: Microscale Analysis of Pyrite (δ34S) and Barite (δ34S, δ18O) in the Canol Formation (Selwyn Basin, Canada). Frontiers in Earth Science, 2022, 9, .	1.8	9
68	Metallogenic Evolution of the Mackenzie and Eastern Selwyn Mountains of Canada's Northern Cordillera, Northwest Territories: A Compilation and Review. Geoscience Canada, 2013, 40, .	0.8	8
69	The Tiger Deposit: A Carbonate-Hosted, Magmatic-Hydrothermal Gold Deposit, Central Yukon, Canada. Economic Geology, 2016, 111, 421-446.	3.8	8
70	In Situ Monazite Dating of Sediment-Hosted Stratiform Copper Mineralization in the Redstone Copper Belt, Northwest Territories, Canada: Cupriferous Fluid Flow Late in the Evolution of a Neoproterozoic Sedimentary Basin. Economic Geology, 2017, 112, 1773-1806.	3.8	8
71	The mineralogical and lithogeochemical footprint of the George Fisher Zn-Pb-Ag massive sulphide deposit in the Proterozoic Urquhart Shale Formation, Queensland, Australia. Chemical Geology, 2021, 560, 119975.	3.3	8
72	Laser ablation split stream for <i>in situ</i> sulfur isotope and elemental analysis. Journal of Analytical Atomic Spectrometry, 2021, 36, 1118-1124.	3.0	8

#	Article	IF	CITATIONS
73	Origin of sulfur and crustal recycling of copper in polymetallic (Cu-Au-Co-Bi-U±ÂAg) iron-oxide-dominated systems of the Great Bear Magmatic Zone, NWT, Canada. Mineralium Deposita, 2018, 53, 353-376.	4.1	5
74	Diagenetic Controls on the Formation of the Anarraaq Clastic-Dominated Zn-Pb-Ag Deposit, Red Dog District, Alaska. Economic Geology, 2021, 116, 1803-1824.	3.8	5
75	Microthermometry and noble gas isotope analysis of magmatic fluid inclusions in the Kerman porphyry Cu deposits, Iran: constraints on the source of ore-forming fluids. Mineralium Deposita, 2022, 57, 155-185.	4.1	4
76	Hydrodynamic Constraints on Ore Formation by Basinâ€Scale Fluid Flow at Continental Margins: Modelling Zn Metallogenesis in the Devonian Selwyn Basin. Geochemistry, Geophysics, Geosystems, 2021, 22, e2020GC009453.	2.5	3
77	Using whole rock and in situ pyrite chemistry to evaluate authigenic and hydrothermal controls on trace element variability in a Zn mineralized Proterozoic subbasin. Geochimica Et Cosmochimica Acta, 2022, 318, 366-387.	3.9	3
78	The geology of the carbonate-hosted Blende Ag–Pb–Zn deposit, Wernecke Mountains, Yukon, Canada. Mineralium Deposita, 2015, 50, 83-104.	4.1	2
79	Constraints on the source and evolution of mineralising fluids in the Norrbotten Fe oxide-Cu-Au province, Sweden. , 2005, , 825-828.		0
80	Acceptance of the SEG Waldemar Lindgren Award for 2007. Economic Geology, 2008, 103, 1386-1387.	3.8	0